

A Nonclassical Dihydrogen Adduct of $S = 1/2$ Fe(I)Yunho Lee,^{†,§} R. Adam Kinney,^{‡,||} Brian M. Hoffman,^{*,‡} and Jonas C. Peters^{*,†}[†]Division of Chemistry and Chemical Engineering, California Institute of Technology, Pasadena, California 91125, United States[‡]Department of Chemistry, Northwestern University, 2145 Sheridan Road, Evanston, Illinois 60208, United States

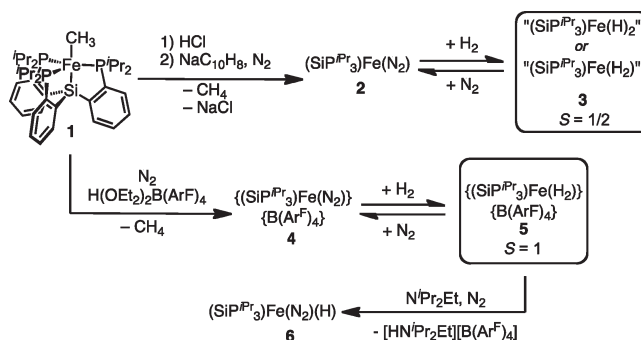
§ Supporting Information

ABSTRACT: We have exploited the capacity of the $(\text{SiP}^{\text{IPr}}_3)\text{Fe}(\text{I})$ scaffold to accommodate additional axial ligands and characterized the mononuclear $S = 1/2$ H_2 adduct complex $(\text{SiP}^{\text{IPr}}_3)\text{Fe}^{\text{I}}(\text{H}_2)$. EPR and ENDOR data, in the context of X-ray structural results, revealed that this complex provides a highly unusual example of an open-shell metal complex that binds dihydrogen as a ligand. The H_2 ligand at 2 K dynamically reorients within the ligand-binding pocket, tunneling among the energy minima created by strong interactions with the three Fe–P bonds.

Low-valent iron has been proposed to play a prominent role in the function of hydrogenase and nitrogenase enzymes, a hypothesis that has inspired the study of formally low-valent iron model complexes that afford access to N_2 and H_2 ligation.^{1–3} Whereas model systems have historically focused on Fe(0) and Fe(II) systems in this context, the coordination chemistry of Fe(I) has more recently come into focus.⁴ This is in part due to its suggested intermediacy in enzymatic hydrogenase activity. Fe(I) is a key formal oxidation state to consider for N_2 and H^+ reduction cycles, and understanding interactions between Fe(I) and N_2/H_2 is essential.

In several recent studies using a tripodal tetradenate tris-(phosphino)silyl ligand XL_3 (e.g., $\text{SiP}^{\text{IPr}}_3 = [\text{Si}(o\text{-C}_6\text{H}_4\text{P}^{\text{IPr}})_3]^-$),^{3b,4} it has been established that five-coordinate iron in a trigonal-bipyramidal (TBP) geometry ($\text{XL}_3\text{Fe}-\text{L}'$) can accommodate a terminally bonded N_2 (or CO) ligand in the axial site across three formal oxidation states ($\text{XL}_3\text{Fe}^0-\text{N}_2^-$, $\text{XL}_3\text{Fe}^{\text{I}}-\text{N}_2$, and $\text{XL}_3\text{Fe}^{\text{II}}-\text{N}_2^+$). It is noteworthy that the spin states of these TBP systems vary such that an $S = 0$ state is favored for Fe(0), an $S = 1/2$ state for Fe(I), and an $S = 1$ state for Fe(II). These findings encouraged us to explore the affinity of dihydrogen for the axial site, particularly for the $S = 1/2$ Fe(I) or $S = 1$ Fe(II) states. Whereas it is common for H_2 to occupy the same coordination site as N_2 , thoroughly characterized dihydrogen adducts of open-shell complexes for transition metals remain exceptionally rare.^{5,6} Oxidative addition to form a dihydride and heterolytic cleavage to form a monohydride are well-established alternatives. NMR techniques, including measurement of T_1 values and J_{HD} coupling constants, have been the methods of choice for characterizing closed-shell H_2 adducts and distinguishing between the dihydrogen/dihydride extrema on the H_2 bonding continuum.⁷ Open-shell H_2 adduct complexes are not amenable to this approach because of the extreme line broadening of resonances expected for H atoms directly coordinated to a metal center with spin $S > 0$. Because the $S = 1/2$ state is EPR-active, we reasoned that a combined electron paramagnetic

Scheme 1



resonance (EPR)/electron–nuclear double resonance (ENDOR) study might prove most effective in characterizing the product formed by reaction of H_2 with the $S = 1/2$ Fe(I) complex. The present report provides the results of such a study and introduces an $S = 1/2$ $\text{Fe}^{\text{I}}(\text{H}_2)$ adduct complex. Evidence for its related but cationic $S = 1$ $\text{Fe}^{\text{II}}(\text{H}_2)^+$ analogue is also provided.

As previously reported, treatment of the methyl complex $(\text{SiP}^{\text{IPr}}_3)\text{Fe}-\text{CH}_3$ (**1**) with HCl followed by reduction generates the $S = 1/2$ Fe(I)– N_2 adduct $(\text{SiP}^{\text{IPr}}_3)\text{Fe}(\text{N}_2)$ (**2**).^{4a,b} The N_2 ligand is sufficiently labile to be displaced by H_2 in benzene to afford a yellow species formulated as $S = 1/2$ “ $(\text{SiP}^{\text{IPr}}_3)\text{Fe}(\text{H}_2)$ ” or “ $(\text{SiP}^{\text{IPr}}_3)\text{Fe}(\text{H}_2)$ ” (**3**) ($\mu_{\text{eff}} = 1.9 \mu_{\text{B}}$ by the Evans method; Scheme 1) in nearly quantitative yield. The optical spectrum of **3** [see the Supporting Information (SI)] features a low-energy d–d transition at 1350 nm ($\epsilon \approx 100 \text{ cm}^{-1} \text{ M}^{-1}$) similar to that of **2** (1250 nm, $\epsilon \approx 300 \text{ cm}^{-1} \text{ M}^{-1}$).

Displacement of the N_2 ligand of **2** by H_2 can be conveniently monitored by ^1H NMR spectroscopy in C_6D_6 (Figure 1). As shown in Figure 1, the H_2 adduct **3** is stable to vacuum over prolonged periods (even at 60 °C over 12 h) but converts back to **2** upon exposure to N_2 , which would be consistent with an associative exchange process proceeding through a formally 19-electron intermediate. Alternatively, and perhaps more likely, is a process wherein a labile phosphine donor exposes a site for N_2 binding via a 15-electron intermediate, followed by H_2 loss and recoordination of the phosphine donor to provide **2**. We also prepared and similarly characterized the D_2 derivative of **3** (see the SI). The ^1H NMR spectrum of **3-D}_2 is analogous to that for **3**, and an ^2H NMR spectrum does not reveal any deuterium resonances for **3-D}_2** (see the SI). This fact is consistent with deuterons that are directly bonded to an $S = 1/2$ iron center.**

Received: July 26, 2011

Published: September 28, 2011

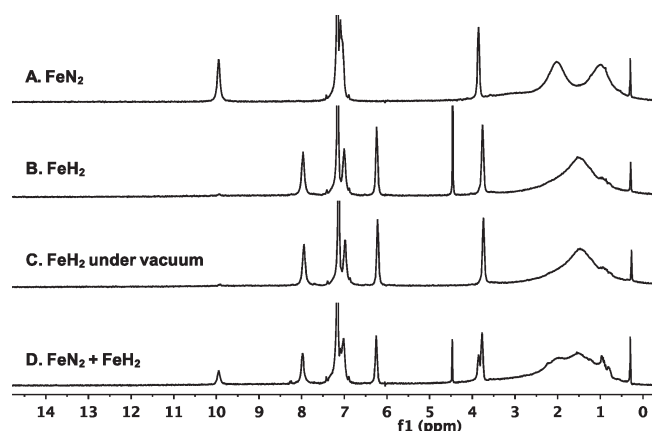


Figure 1. ^1H NMR spectra of (A) $(\text{SiP}^{\text{iPr}}_3)\text{Fe}(\text{N}_2)$ (**2**), (B) $(\text{SiP}^{\text{iPr}}_3)\text{Fe}(\text{H}_2)$ (**3**), (C) **3** under full vacuum, and (D) a mixture of **2** and **3** measured in C_6D_6 at RT.

Incubation of **2** under HD instead of H_2 at RT for 15 h caused no HD/ H_2 / D_2 scrambling, suggesting that **3** binds an intact H_2 ligand rather than undergoing heterolytic activation (e.g., to generate a Si—H or P—H bond and an Fe—H bond).

The well-behaved NMR properties of **2** and **3** allow for the direct measurement of the equilibrium constant for H_2/N_2 exchange at the $S = 1/2$ Fe center. Using sealed J-Young vessels with known N_2/H_2 gas mixtures and exploiting the well-defined resonances of the $\text{SiP}^{\text{iPr}}_3$ ligand at ca. 10 and 8 ppm to integrate the respective concentrations of **2** and **3**, we estimated the equilibrium constant to be 50 ± 20 in favor of H_2 binding in C_6D_6 at room temperature.

X-ray structures of **3** were obtained from crystals under vacuum and under an atmosphere of H_2 . While both structures are of high quality, neither shows the positions of the H_2 /hydride. Nonetheless, it is clear that the two structures are essentially identical and are likewise very similar to that of the N_2 adduct complex **2**^{4b} and its CO congener $(\text{SiP}^{\text{iPr}}_3)\text{Fe}^{\text{I}}(\text{CO})$ ^{4c} (Figure 2 and Table 1), except for the absence of an axially bound diatomic ligand for **3**. We were unable to locate a vibration consistent with either an Fe—H or an Fe—(H—H) motif. Whereas terminal M—H vibrations are readily assigned, $\nu(\text{H—H})$ vibrations for H_2 adduct complexes are not as reliably discerned.^{6a,7} The absence of $\nu(\text{Si—H})$ or $\nu(\text{P—H})$ stretches in the IR spectrum is likewise inconsistent with heterolytic generation of Fe—H and Si—H/P—H bonds but consistent with an intact H_2 ligand.

We examined the EPR spectrum of **3** in both the solid state and as a frozen glass. Treatment of **2** ($g = [2.364, 2.036, 2.003]$) with H_2 gas leads to complete loss of the starting material and the appearance of **3** with an $S = 1/2$ EPR signal ($g = [2.275, 2.064, 2.015]$), as measured for frozen solutions (9:1 THF/Me-THF) and pure powders (see the SI). The unique magnetic direction g_1 ($g_1 = 2.275$) is assigned to the pseudo- C_3 symmetry axis of the molecule. These low-temperature measurements of **3**, combined with NMR Evans method (Table 1) show that the coordination sphere and low-spin d^7 character of the Fe(I) center are maintained under all conditions.

The g values of **3** (and **2**) can be described in terms of a “pseudo-Jahn–Teller” (PJT) effect wherein spin–orbit coupling competes with vibronic coupling to lower the energy of the molecule by a distortion from a C_3 -symmetric structure.⁸ The idealized trigonal Fe(I) geometry created by the $[\text{SiP}^{\text{iPr}}_3]^-$ ligand leads to a doubly

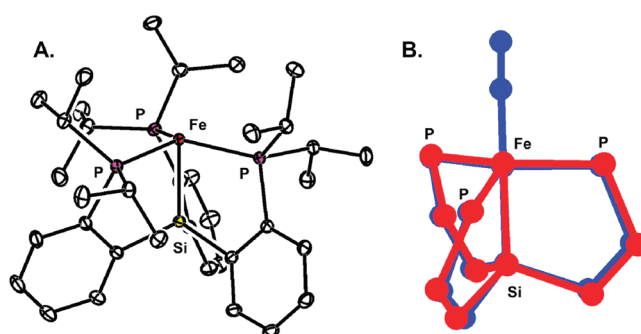


Figure 2. (A) Displacement ellipsoid (50%) representation of **3** obtained from a crystal grown under a H_2 atmosphere. H atoms of $\text{SiP}^{\text{iPr}}_3$ have been omitted for clarity. (B) Overlay of the closely related core structures of **2** (blue) and **3** (red).

Table 1. Selected Data for Complexes Discussed in the Text

complex	$d_{\text{Fe—Si}}$ (Å)	$d_{\text{Fe—P}}$ (Å)	$\angle \text{PFeP}$ (deg)	μ_{eff} (μ_B) ^a
$\text{Fe}(\text{N}_2)$ 2	2.2713(6)	2.2657(5)	111.82(2)	1.90
		2.2841(7)	113.59(2)	
		2.3244(6)	128.64(2)	
$\text{Fe}(\text{H}_2)$ 3 ^b	2.254(1)	2.2442(9)	113.31(3)	1.88
		2.260(1)	118.07(3)	
		2.2631(9)	122.36(4)	
$\text{Fe}(\text{H}_2)$ 3 ^c	2.2478(3)	2.2418(3)	113.157(9)	
		2.2577(3)	117.63(1)	
		2.2613(2)	123.16(1)	

^a Magnetic moments by the Evans method in C_6D_6 at 22 °C. ^b Under vacuum. ^c Under H_2 .

degenerate ^2E ground state in which the $(d_{xy}, d_{x^2-y^2})$ orbital doublet is triply occupied, and therefore, the complex is subject to a JT distortion. The most obvious distortion in the X-ray structure of **3** (and **2**) is in the P—Fe—P angles, with an increase in one angle from the symmetric value of 120° and a decrease in the other two (e.g., for **3**, $\text{P2—Fe—P3} = 123.2^\circ$ and $\text{P1—Fe—P3} \approx \text{P1—Fe—P2} \approx 115.4^\circ$).

Although the hydrogenic ligand of **3** is not visible by X-ray diffraction (XRD), we directly characterized this ligand by ^1H ENDOR spectroscopy. Figure 3 displays a part of the 2D field–frequency ^1H ENDOR pattern comprising spectra collected across the EPR envelope of **3**. The spectrum collected at g_3 shows a doublet centered at the ^1H Larmor frequency that is split by the hyperfine interaction $|A_3(^1\text{H})| = 37.8$ MHz. The equivalent ^2H ENDOR spectrum from $[\text{SiP}^{\text{iPr}}_3]\text{Fe}(^2\text{H}_2)$ (**3'**) shows a corresponding doublet; its splitting, $|A_3(^2\text{H})| = 5.6$ MHz, matches that of the ^1H doublet upon scaling by the respective nuclear g values with a small isotope-effect correction. Likewise, the 2D field–frequency pattern of the ^2H ENDOR spectra corresponds to the ^1H pattern of Figure 3 (see the SI). The complete 2D pattern is exceptionally well simulated by hyperfine coupling to a *single type* of ^1H , with coupling tensor $\mathbf{A} = [+2.3, -40.6, -37.8]$ MHz, isotropic coupling $a_{\text{iso}} = -25.4$ MHz, and anisotropic dipolar hyperfine coupling tensor $\mathbf{T} = [+27.7, -15.2, -12.4]$ MHz; the tensor orientation relative to g is given by the rotation angles $(\alpha, \beta, \gamma) = (0, 6, 0)$. The absolute sign of the ^1H hyperfine coupling was determined experimentally using the PESTRE technique (see the SI).⁹

The simplest chemical species compatible with a single type of interacting ^1H whose Fe—H vector lies close to g_1 is a neutral

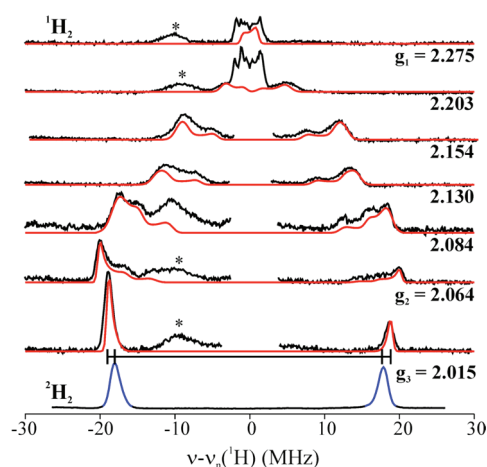


Figure 3. Q-band stochastic 2D field–frequency continuous-wave ENDOR pattern for **3** (black) with simulations of the exogenous “H₂” ¹H ENDOR response (red; see the text for details). The corresponding ²H ENDOR spectrum collected from 3-D₂ at g₃ = 2.015 (blue) is scaled by the ratio of the ¹H and ²H nuclear g values. ENDOR responses from ³¹P of the [SiP^{ᵀᵀᵀ}][−] ligand are indicated by (*).

complex in which a terminal hydride bound to Fe(I) is generated by heterolytic cleavage of the H₂ molecule with delivery of the proton to the Si of the SiP^{ᵀᵀᵀ} ligand. However, this model requires cleavage of the Fe–Si bond with rearrangement of the geometry at Si and a substantial increase in *d*_{Fe–Si} relative to **2**, whereas the crystal structure of **3** reveals a negligible change in *d*_{Fe–Si} relative to **2** (see above).¹⁰ This conclusion was corroborated by EPR measurements showing that the solution, polycrystalline powder (see the SI), and single-crystal forms of **3** have the same g tensor¹¹ and thus the same structure. The ENDOR pattern of Figure 3 must therefore arise from a neutral complex that has been generated by the addition of H₂, either in the form of an Fe(I)–H₂ complex or via oxidative addition to an Fe(III) dihydride.

The observed g values provide a powerful argument against the formulation of **3** as an Fe(III) dihydride. The PJT effect predicts that the g values for an Fe(III) d⁵ ion must be less than g_e = 2, contrary to observation.¹²

Elimination of the Fe(III) dihydride model for **3** was confirmed by analysis of the ¹H ENDOR results. The 2D ENDOR pattern for **3** can be compared with that predicted for this species on the basis of a consensus geometry of similar complexes (*d*_{H–H} > 1.6 Å; *d*_{Fe–H} = 1.54 Å; Figure 4).¹³ The critical parameter in the ENDOR simulations is the value of the angle β between the g₁ principal axis and the Fe–H vectors. In an Fe(III) dihydride complex, β ≥ 30°. ¹H ENDOR simulations using β ≈ 30° (Figure 4B, β = 30°; also see the SI) showed this to be incompatible with experiment. Figure 4B illustrates this with simulations for a spectrum collected at a field where each component of the doublet observed at g₃ (and g₂) in Figure 3 is split into an intense peak and a less intense “shoulder”. The splitting for β ≈ 30° is far larger than seen experimentally.

Rejection of the assignment of **3** as an Fe(I) monohydride or an Fe(III) dihydride implies by elimination that **3** is an Fe(I)–H₂ adduct. The similarity of the solution NMR and UV–vis data for **2** and **3** are also highly consistent with this notion (see above). The ENDOR simulations further show that even at 2 K, the H₂ of the Fe(I)–H₂ adduct undergoes dynamic reorientation within the ligand-binding pocket of **3**. In a consensus geometry for the

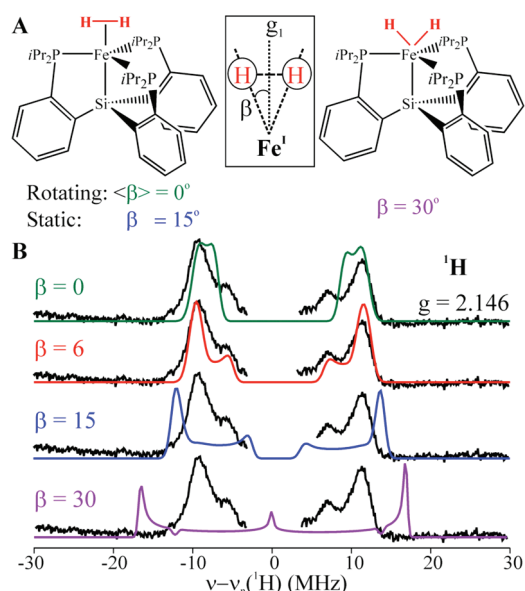


Figure 4. Simulations of ¹H ENDOR spectra for models of **3**, for the spectrum at g = 2.146. The simulations are based on the hyperfine tensor determined through a fit to the 2D field–frequency plot of Figure 3 (A = [2.3, −40.6, −37.8] MHz) but with the dipolar interaction rotated by the angle β between the H nuclei and the g₁ axis, which is taken to lie along the Fe–Si bond (labeled as “g₁”).

Fe(I)–H₂ center (*d*_{H–H} = 0.85 Å; *d*_{Fe–H} = 1.62 Å),¹⁴ the H atoms would exhibit a geometrically determined β value of ~15°. As shown in Figure 4 (also see the SI), the 2D ENDOR pattern of Figure 3 cannot be described by such a static structure. The electron–nuclear dipolar interaction for H₂ must therefore be modulated by rapid reorientation of H₂ about the Fe–H₂ bond axis.

The H₂ cannot undergo rotation that is only weakly hindered by the binding pocket environment because in that case the ground state would correspond to the free-rotor ground rotational state (*m* = 0).¹⁵ The total wave function of a rotating ¹H₂ must be antisymmetric with respect to exchange of the two ¹H nuclei. For ¹H₂ bound to the Fe(I) center of a statically distorted **3**, this wave function is the product of the ¹H₂ rotational and spin functions. The rotor ground state is symmetric with respect to exchange of the two H nuclei (the “para” state) and thus must be associated with the antisymmetric *I* = 0 total nuclear spin state, which cannot exhibit a ¹H ENDOR signal.¹⁶ If **3** instead undergoes a dynamic PJT distortion, the total H₂ wave function would have the vibronic electron–nuclear wave function as an additional factor. For **3** this factor is symmetric with respect to exchange, so the conclusion remains.

Instead, the measurements are probably best understood as a consequence of H₂ tunneling among localized states set up by a strong sixfold barrier associated with rotation of the “dumbbell-shaped” H₂ within the threefold-symmetric molecular potential (Figure 5).⁵ In this limit, the ¹H ENDOR response is allowed, and tunneling would average the dipolar interaction, causing the unique hyperfine axis to lie along the axis of rotation. We attribute the nonzero β to tensor noncollinearity caused by the distortion from trigonal symmetry that is introduced by the PJT effect and observed in the X-ray structure (Table 1).

It is of interest to compare the stable (SiP^{ᵀᵀᵀ})Fe^I(H₂) complex described here to that assigned as a dihydrogen adduct of Mo(III), “[HIPTN₃N]Mo^{III}(H₂)”.^{6b} In a recent report, it was shown that the latter species undergoes facile heterolytic cleavage of H₂,

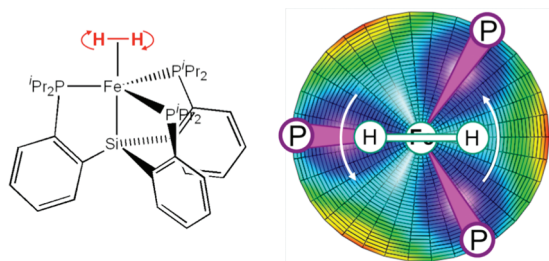


Figure 5. Schematic representation of H_2 hopping/tunneling on the potential energy surface for PJT-distorted **3**.

delivering H^- to Mo to afford $[[\text{HIPTN}_3\text{N}]\text{Mo}^{\text{III}}(\text{H})]^-$ and H^+ , with the H^+ presumably delivered to sacrificial $[\text{HIPTN}_3\text{N}]^{3-}$ at reduced temperature.^{6c} In contrast, the Si atom of the $(\text{SiP}^{\text{iPr}}_3)\text{Fe}$ scaffold is insufficiently basic to accept H^+ from the coordinated H_2 , thus stabilizing the H_2 adduct complex **3** against heterolytic cleavage. The stability of H_2 bound to the “ $(\text{SiP}^{\text{iPr}}_3)\text{Fe}$ ” scaffold also extends to its corresponding cation, “ $(\text{SiP}^{\text{iPr}}_3)\text{Fe}^+$ ”. Treating previously reported $S = 1$ $\{(\text{SiP}^{\text{iPr}}_3)\text{Fe}(\text{N}_2)\}\{\text{BAr}^{\text{F}}_4\}$ (**4**) with H_2 reversibly generates what we have assigned as the $S = 1$ complex $\{(\text{SiP}^{\text{iPr}}_3)\text{Fe}(\text{H}_2)\}\{\text{BAr}^{\text{F}}_4\}$ (**5**) (Scheme 1). Complex **5** is EPR/ENDOR-silent because of its integer-spin triplet state, but solution NMR and UV–vis data (see the SI) provide evidence for a species that is highly similar to the cationic N_2 adduct **4**. Moreover, addition of an exogenous base (e.g., $\text{N}^{\text{iPr}}_2\text{Et}$) to **5** under N_2 cleanly effects heterolytic cleavage, affording the neutral $\text{Fe}(\text{II})$ complex $(\text{SiP}^{\text{iPr}}_3)\text{Fe}(\text{N}_2)(\text{H})$ (**6**) (Scheme 1).

In summary, the mononuclear $S = 1/2$ $\text{Fe}^{\text{I}}(\text{H}_2)$ adduct complex **3** provides a highly unusual example of a well-characterized open-shell metal complex that binds dihydrogen as a ligand. Combined XRD, EPR, and ENDOR data are consistent with a PJT-distorted d^7 configuration and a H_2 ligand that at 2 K tunnels among the energetic minima created by the $\text{Fe}–\text{P}$ bonds. The $S = 1/2$ title complex $(\text{SiP}^{\text{iPr}}_3)\text{Fe}(\text{H}_2)$ can be formally oxidized to its $S = 1$ cation, $\{(\text{SiP}^{\text{iPr}}_3)\text{Fe}(\text{H}_2)\}^+$, and the latter species binds H_2 as an intact ligand that is subject to heterolytic cleavage upon addition of exogenous base.

■ ASSOCIATED CONTENT

S **Supporting Information.** Experimental procedures, characterization and crystallographic data. This material is available free of charge via the Internet at <http://pubs.acs.org>.

■ AUTHOR INFORMATION

Corresponding Author

bmh@northwestern.edu; jpeters@caltech.edu

Present Addresses

[§]Department of Chemistry, School of Molecular Science, Korea Advanced Institute of Science and Technology, Daejeon, Republic of Korea.

Author Contributions

^{||}These authors contributed equally.

■ ACKNOWLEDGMENT

We acknowledge the NIH (GM-070757 to J.C.P.; HL 13531 to B.M.H.). We thank Prof. Harden McConnell for insightful

suggestions about low-temperature dynamics. Dr. Peter Müller provided assistance with XRD analyses. Professor George R. Rossman provided access to a near-IR spectrometer. Henry Fong probed the deprotonation of **5**.

■ REFERENCES

- (1) (a) Tard, C.; Pickett, C. J. *Chem. Rev.* **2009**, *109*, 2245. (b) Gloaguen, F.; Rauchfuss, T. B. *Chem. Soc. Rev.* **2009**, *38*, 100. (c) Vincent, K. A.; Parkin, A.; Armstrong, F. A. *Chem. Rev.* **2007**, *107*, 4366.
- (2) (a) Smith, J. M.; Lachiotte, R. J.; Pittard, K. A.; Cundari, T. R.; Rodgers, K. R.; Lukat-Rodgers, G.; Lachiotte, R. J.; Flaschenriem, C. J.; Vela, J.; Holland, P. L. *J. Am. Chem. Soc.* **2006**, *128*, 756. (b) Holland, P. L. *Can. J. Chem.* **2005**, *83*, 296.
- (3) (a) Betley, T. A.; Peters, J. C. *J. Am. Chem. Soc.* **2004**, *126*, 6252. (b) Mankad, N. P.; Whited, M. T.; Peters, J. C. *Angew. Chem., Int. Ed.* **2007**, *46*, 5768. (c) Brown, S. D.; Betley, T. A.; Peters, J. C. *J. Am. Chem. Soc.* **2003**, *125*, 322.
- (4) (a) Lee, Y.; Mankad, N. P.; Peters, J. C. *Nat. Chem.* **2010**, *2*, 558. (b) Whited, M. T.; Mankad, N. P.; Lee, Y.; Oblad, P. F.; Peters, J. C. *Inorg. Chem.* **2009**, *48*, 2507. (c) Lee, Y.; Peters, J. C. *J. Am. Chem. Soc.* **2011**, *133*, 4438.
- (5) Kubas, G. J. *Chem. Rev.* **2007**, *107*, 4152.
- (6) For the few cases where H_2 has been suggested to be coordinated to an open-shell metal center, see: (a) Hetterscheid, D. G. H.; Hanna, B. S.; Schrock, R. R. *Inorg. Chem.* **2009**, *48*, 8569. (b) Kinney, R. A.; Hetterscheid, D. G. H.; Schrock, R. R.; Hoffman, B. M. *Inorg. Chem.* **2010**, *49*, 704. (c) Bart, S. C.; Lobkovsky, E.; Chirik, P. J. *J. Am. Chem. Soc.* **2004**, *126*, 13794. (d) Baya, M.; Houghton, J.; Daran, J.-C.; Poli, R.; Male, L.; Albinati, A.; Gutman, M. *Chem.—Eur. J.* **2007**, *13*, 5347.
- (7) (a) Heinekey, D. M.; Lledós, A.; Lluch, J. *Chem. Soc. Rev.* **2004**, *33*, 175. (b) Jessop, P. G.; Morris, R. H. *Coord. Chem. Rev.* **1992**, *121*, 155. (c) Morris, R. H. *Coord. Chem. Rev.* **2008**, *252*, 2381.
- (8) (a) Bersuker, I. B. *The Jahn–Teller Effect*, 1st ed.; Cambridge University Press: Cambridge, U.K., 2006; (b) McNaughton, R. L.; Roemelt, M.; Chin, J. M.; Schrock, R. R.; Neese, F.; Hoffman, B. M. *J. Am. Chem. Soc.* **2010**, *132*, 8645.
- (9) Doan, P. E. *J. Magn. Reson.* **2011**, *208*, 76.
- (10) DFT calculations showed that an isomer with one H atom on Si and on Fe, $(\text{HSiP}^{\text{iPr}}_3)\text{Fe}(\text{H})$, is energetically inaccessible relative to $(\text{SiP}^{\text{iPr}}_3)\text{Fe}(\text{H}_2)$ or $(\text{SiP}^{\text{iPr}}_3)\text{Fe}(\text{H})_2$ isomer.
- (11) Gurbiel, R. J.; Bolin, J. T.; Ronco, A. E.; Mortenson, L.; Hoffman, B. M. *J. Magn. Reson.* **1991**, *91*, 227.
- (12) Ammeter, J. H. *J. Magn. Reson.* **1978**, *30*, 299.
- (13) Cambridge Structural Database (CSD).
- (14) Bruno, I. J.; Cole, J. C.; Edgington, P. R.; Kessler, M.; Macrae, C. F.; McCabe, P.; Pearson, J.; Taylor, R. *Acta Crystallogr.* **2002**, *B58*, 389.
- (15) McConnell, H. M. *J. Chem. Phys.* **1958**, *29*, 1422.
- (16) Eckert, J.; Kubas, G. J. *J. Phys. Chem.* **1993**, *97*, 2378.